



Advancing Compact Light Sources

Giovanni Campri



Elettra Sincrotrone Trieste



Istituto Nazionale di Fisica Nucleare

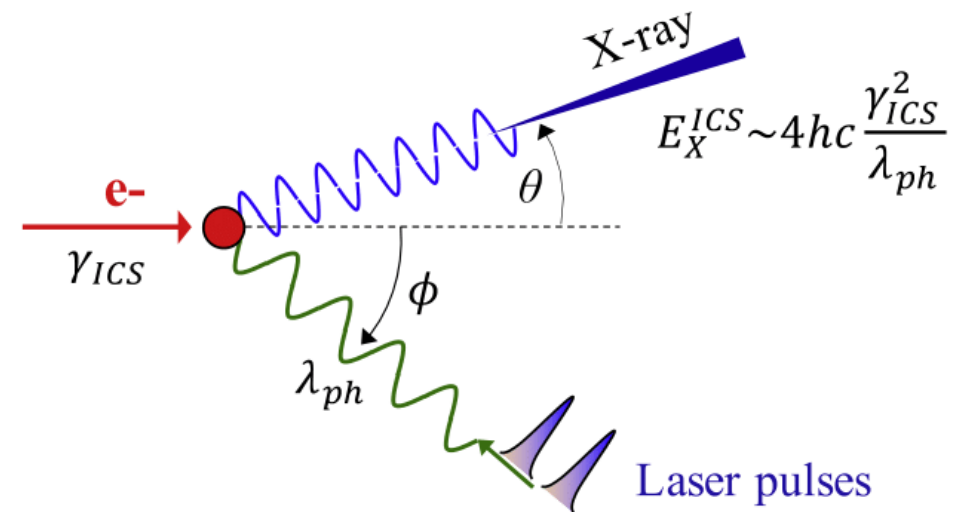
Bologna Compton X-ray Source \longrightarrow ICS-based light source

High quality X-ray beam

- Tunable energy (70-800 keV)
- Quasi-monochromatic
- Short pulses (ps)
- Reasonably high fluxes ($\sim 10^{10}$ ph/s)

Multidisciplinary applications

- Biomedical imaging
- Industrial applications
- Cultural heritage science
- ...and more!



Massimo Placidi, Guest Lawrence Berkeley National Laboratory; massimoplacidi@icloud.com

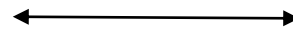
Giovanni Campri, Sapienza University of Rome; giovanni.campri@uniroma1.it

Simone Di Mitri, Elettra-Sincrotrone Trieste; simone.dimitri@elettra.eu

Anna Giribono, **David Alesini**, INFN-LNF; Anna.Giribono@Inf.infn.it (A.G.); david.alesini@Inf.infn.it (D.A.)

Armando Bazzani, **Giorgio Turchetti**, University of Bologna; armando.bazzani@unibo.it (A.B.); giorgio.turchetti@unibo.it (G.T.)

High quality X-ray beam



High quality e-beam

We performed an **electron beam dynamics** study from the photocatode to the IP, in order to design the machine and to obtain a realistic set of parameters to characterise the Compton X-rays.

1° year The photo-injector design (simulated using ASTRA).

2° year The **beam transport and focusing to the IP** design (simulated in elegant CSR included).

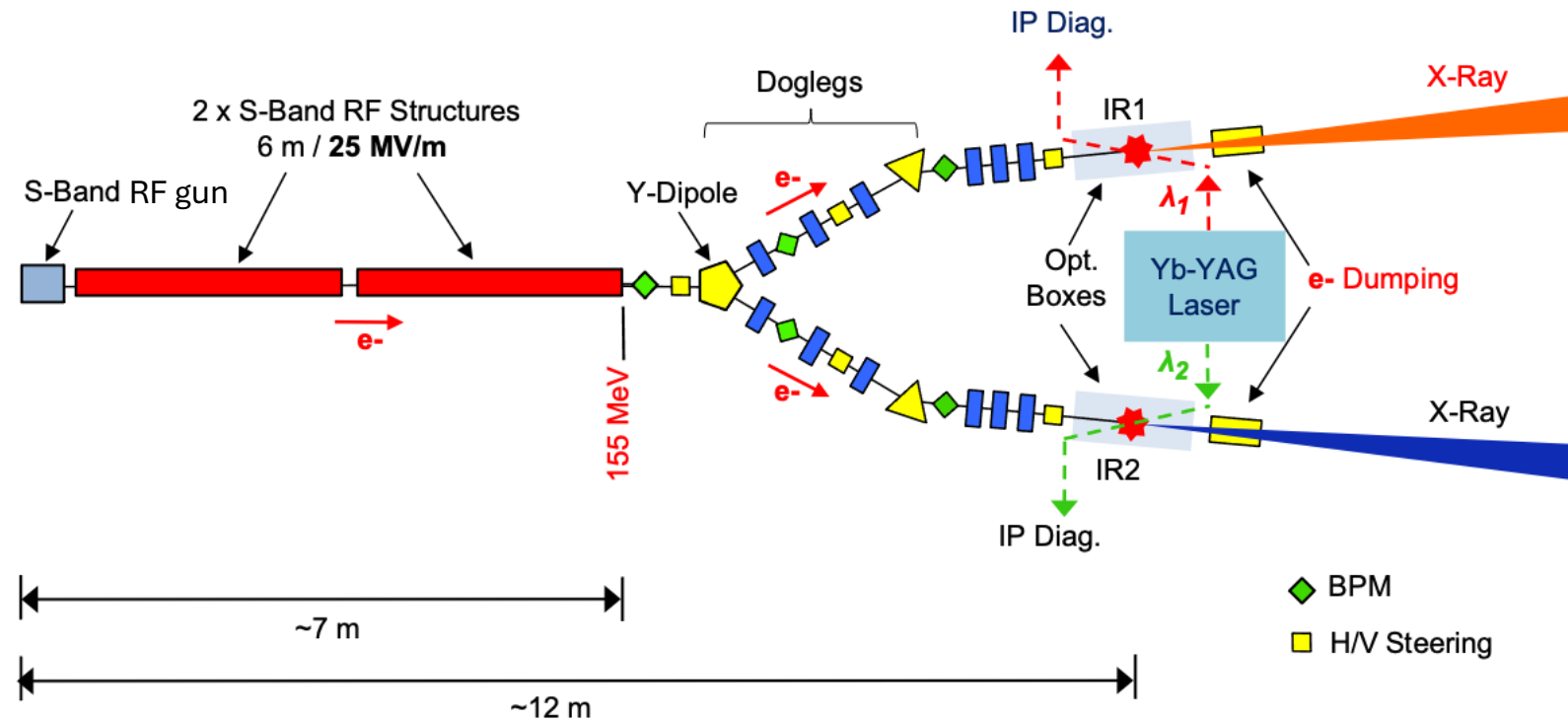


INTERNATIONAL SYMPOSIUM ON
COMPACT SYNCHROTRON X-RAY SOURCES



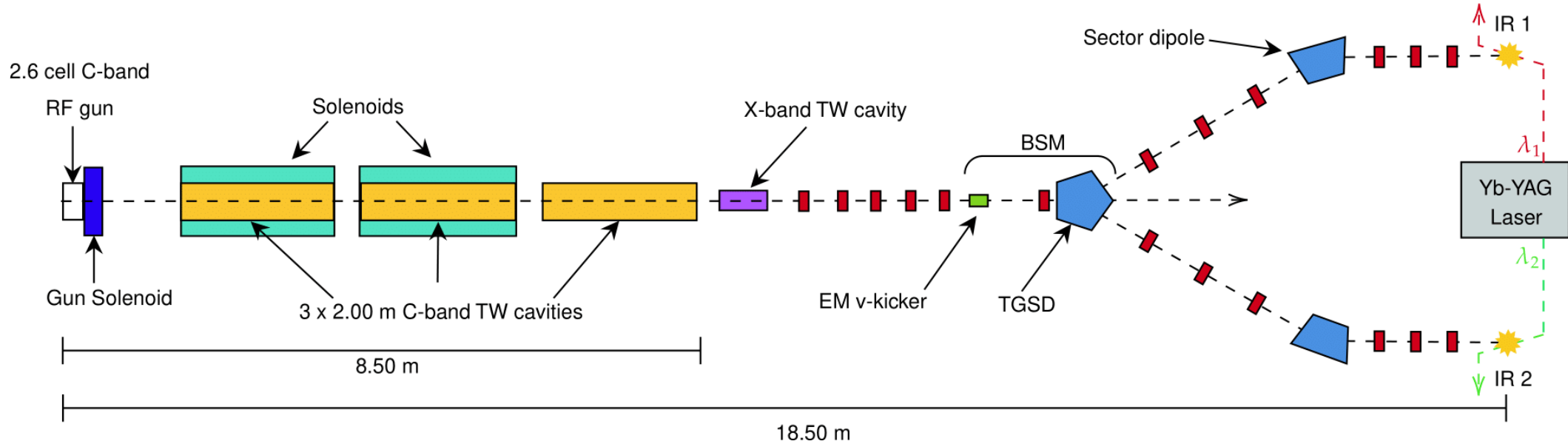
Ultrafast Beams and Applications

BoCXS original design



Original full S-Band configuration of the BoCXS X-ray source. Electron bunches accelerated up to **155 MeV** in an S-Band Linac are transported up to the interaction regions IR1 and IR2 where they interact with photon pulses produced by a laser system operating on the fundamental wavelength ($\lambda_{ph}^0 = 1032 \text{ nm}$) or its 2nd harmonic. ICS X-ray pulses are emitted in two different energy ranges alternatively feeding two user areas.

BoCXS updated layout



BoCXS schematic machine layout (not to scale). These are all the elements included in the beam simulations.

Main upgrades

- Fully redesigned C-band accelerating structure
- X-band linearizer
- Matching section
- BSM in place of the Y-dipole
- A third line for e-beam applications

BoCXS

Bologna Compton X-ray Source

C-band photo-injector

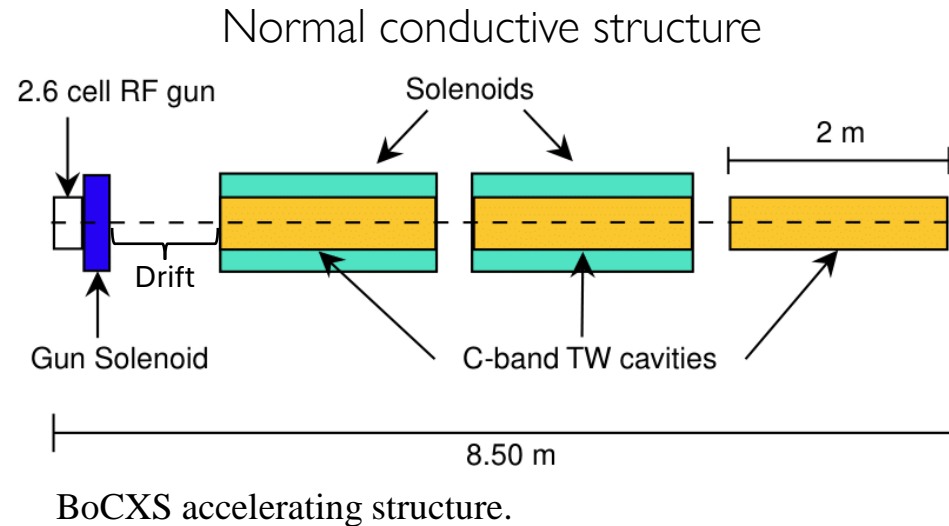


Photo-injector parameters

Parameter	Value
C-band resonant frequency [GHz]	5.712
Rep. rate [kHz]	0.1
Gun peak field [MV/m]	180
TW Cavities peak field [Mv/m]	40

The redesign of the machine led to an even larger footprint.

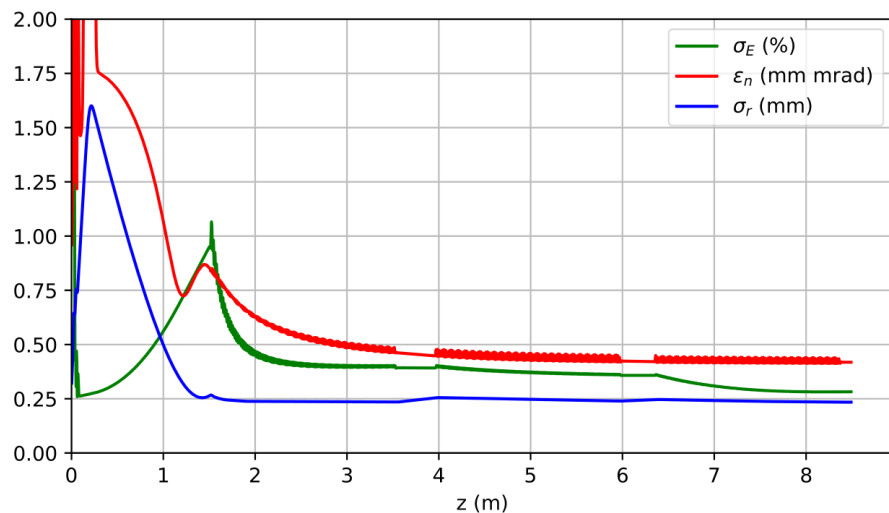
A C-band accelerating structure allows to sustain **higher gradients** at normal conducting temperatures while decreasing the breakdown rate probability, thus **reducing the space** needed for acceleration.

A higher peak field also enhances machine performance in terms of **beam brightness**.



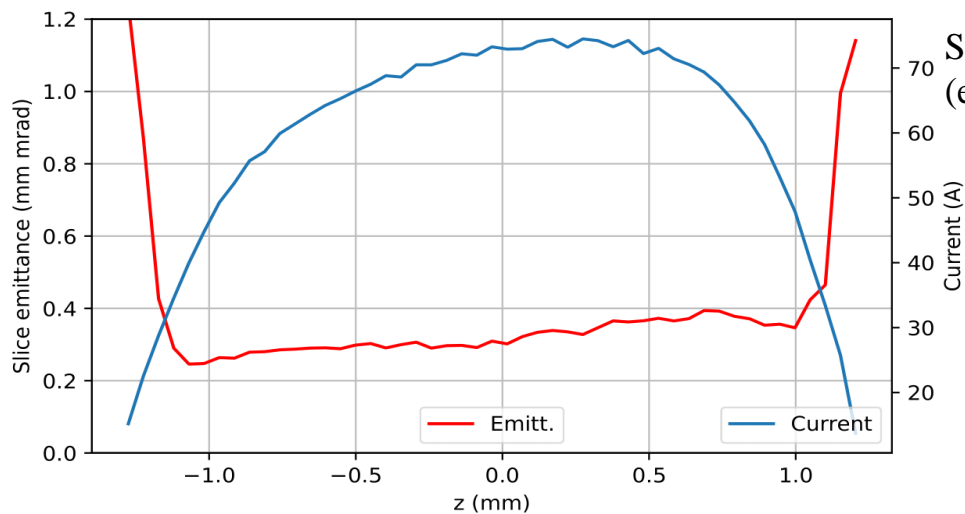
C-band photo-injector optimisation

Simulated with ASTRA (500k particles)



Simulation of beam evolution along the C-band photo-injector.

Photocathode laser



Slice analysis of the beam (end of linac).

Optimised working point parameters for the C-band photo-injector (on-crest operation)

Parameter	Value
Laser rms spot size (Uniform) [mm]	0.3
FWHM length pulse (Flat top) [ps]	8.5
Rise time [ps]	0.5
Beam energy [MeV]	190.3
Bunch charge [nC]	0.5
Norm. proj. emittance [mm mrad]	0.42
Bunch length, rms [ps]	2.1
Transverse beam size, rms [mm]	0.23
Relative energy spread, rms [%]	0.28
Peak current [A]	75

Also the velocity bunching case was studied, although not relevant for BoCXS (IPAC'24)

Linearization with the X-band cavity

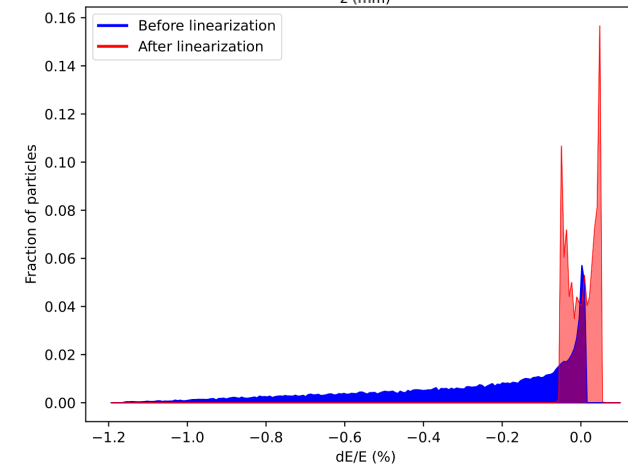
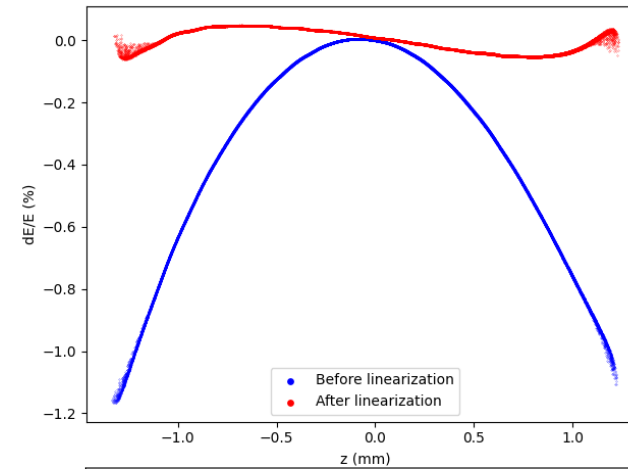
Simulated with elegant (500k particles)

The need for linearization

Effects of chromatic aberrations and CSR on the beam quality

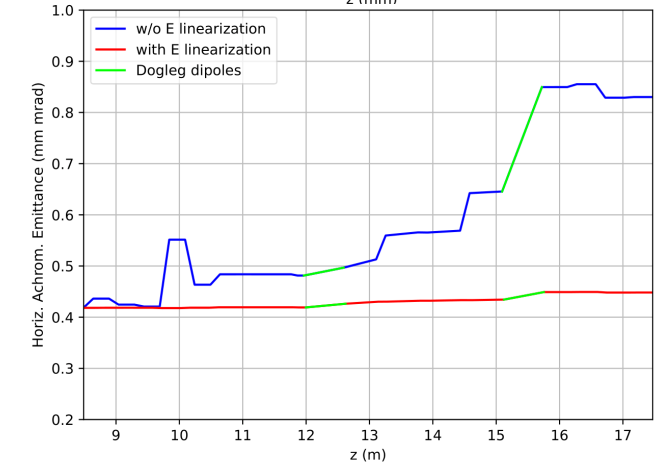
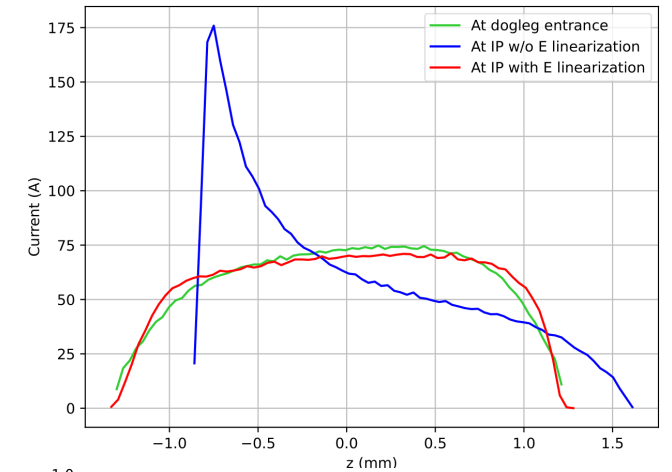
	ε_x [mm mrad]	\hat{I} [A]	σ_E [%]
After linac	0.42	74	0.28
Without linearization			
At IP, CSR OFF	0.59	180	0.28
At IP, CSR ON	0.83	175	0.29
With linearization			
At IP, CSR OFF	0.42	71	0.03
At IP, CSR ON	0.45	71	0.03

Beam longitudinal phase space.



Relative energy distribution.

Beam current.

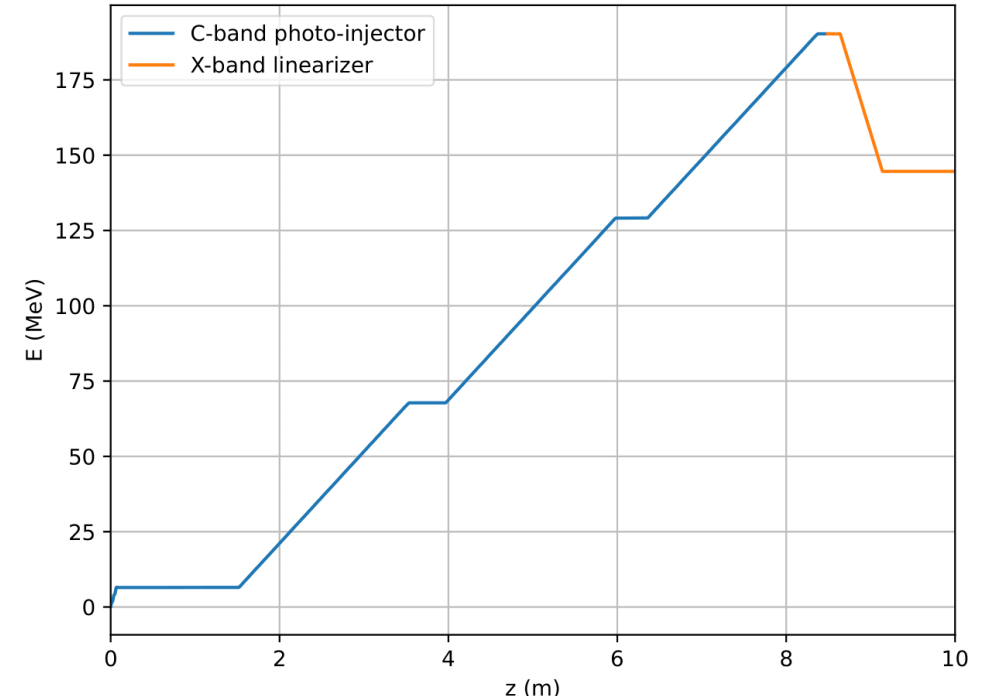


Horizontal achromatic emittance evolution.

Effects of the linearization

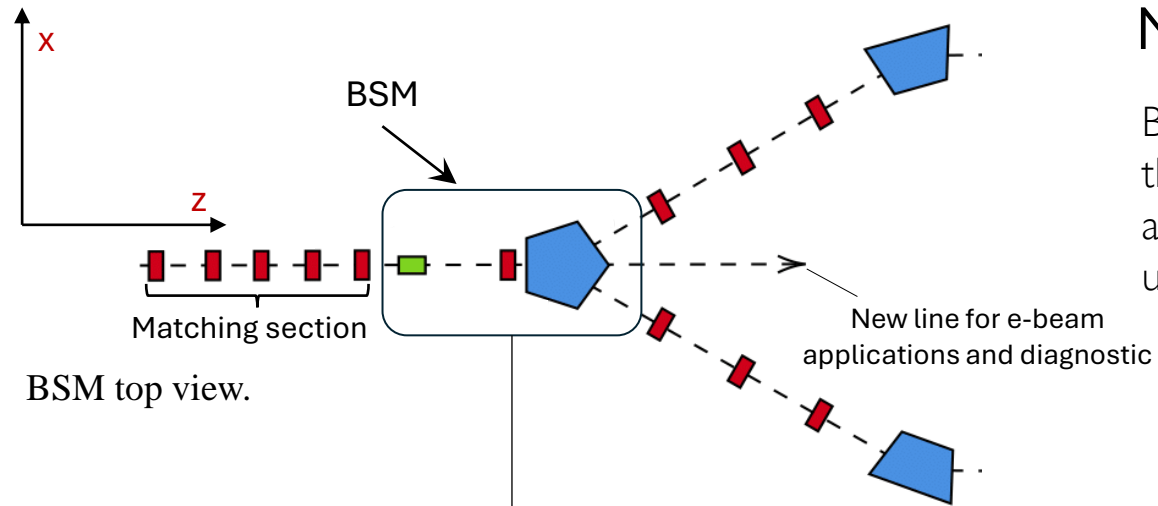
X-band cavity parameters

Parameter	Value
X-band resonant frequency [GHz]	11.424
Rep. rate [kHz]	0.1
X-band cavity field [MV/m]	92.4
Injection phase [deg]	179.72
X-band cavity length [m]	0.5
Beam final relative energy spread, rms [%]	0.03
Beam final energy [MeV]	145



Beam energy evolution along the RF structures. The decelerating effect of the X-band cavity brings the final energy to 145 MeV.

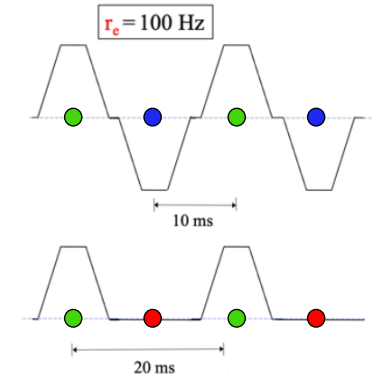
Bunch Selection Module (BSM)



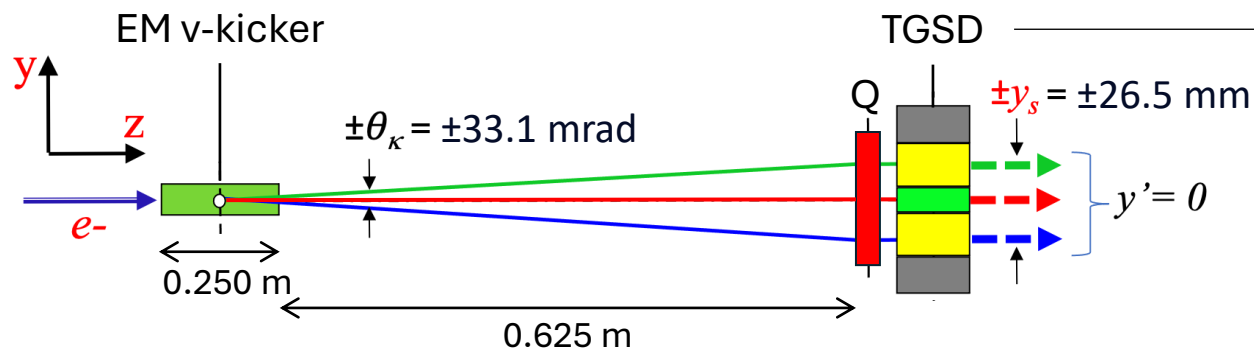
BSM top view.

Multimode operation

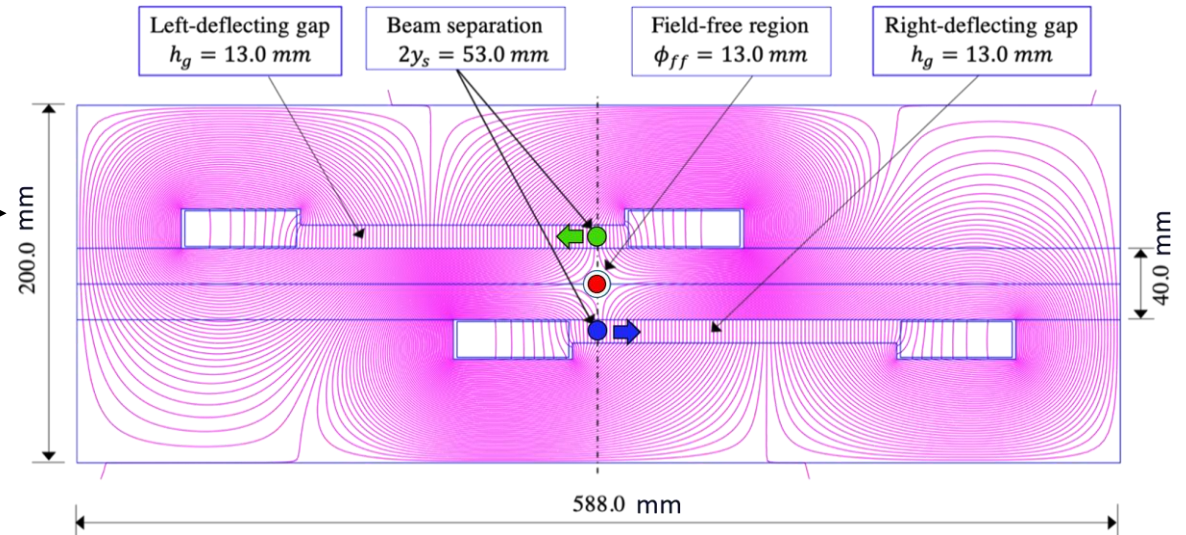
BSM scheme provides the possibility to select the beamline on a bunch-by-bunch basis, allowing a **quasi-simultaneous** operation of up to **three user areas**.



Examples of possible deflecting patterns.

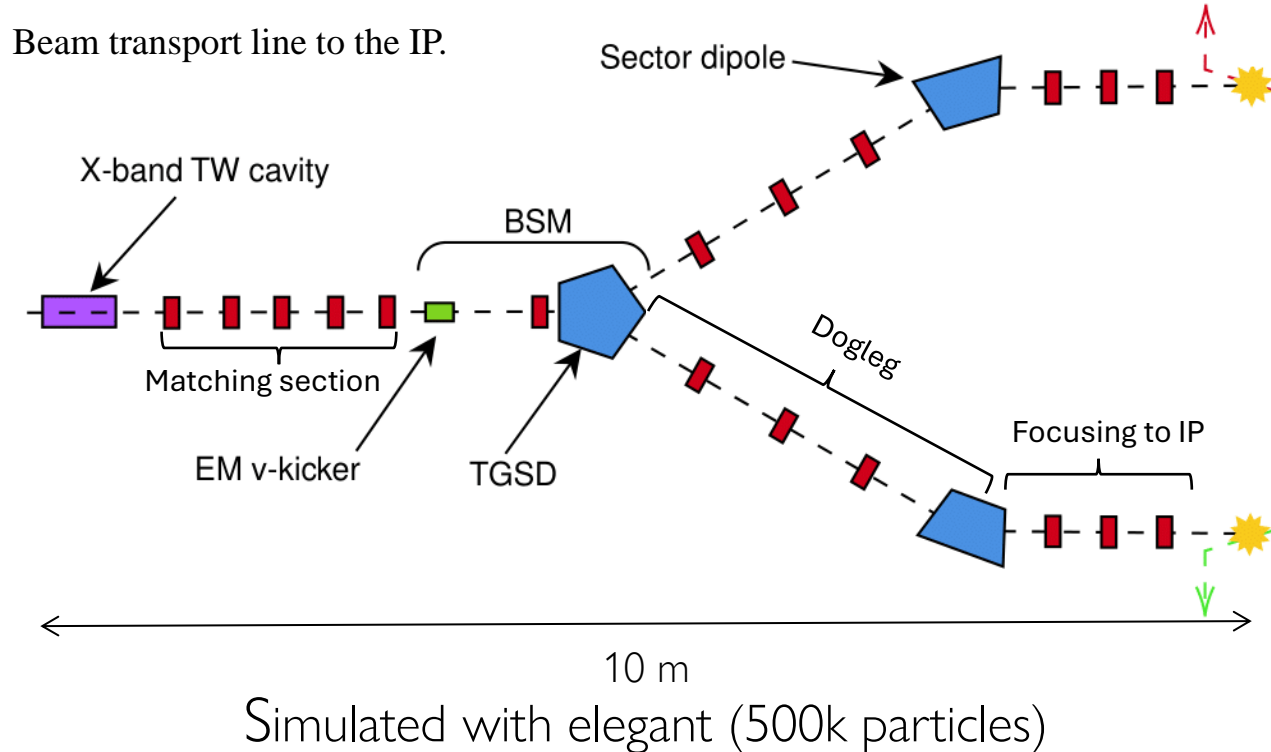


BSM side view.



Front view vertical section of the Poisson-optimized Twin-Gap Septum Dipole (TGSD).

Beam transport and focusing to the IP



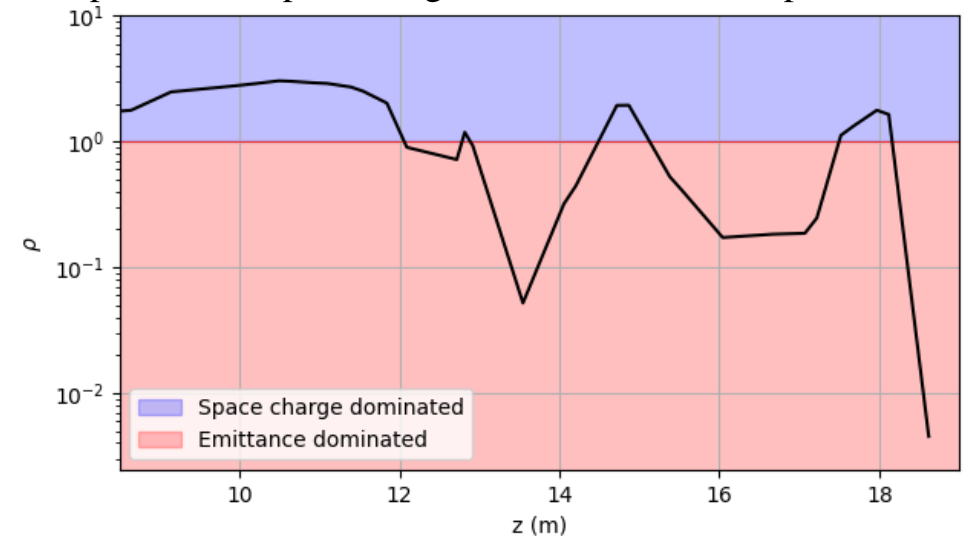
We performed a full **optimisation** of the magnetic lattice using elegant (no space charge).

The the beam dynamics is mostly dominated by the **emittance pressure**.

The **matching section** (a quadrupole quintuplet) is crucial for a proper beam matching to the BSM and the dogleg.

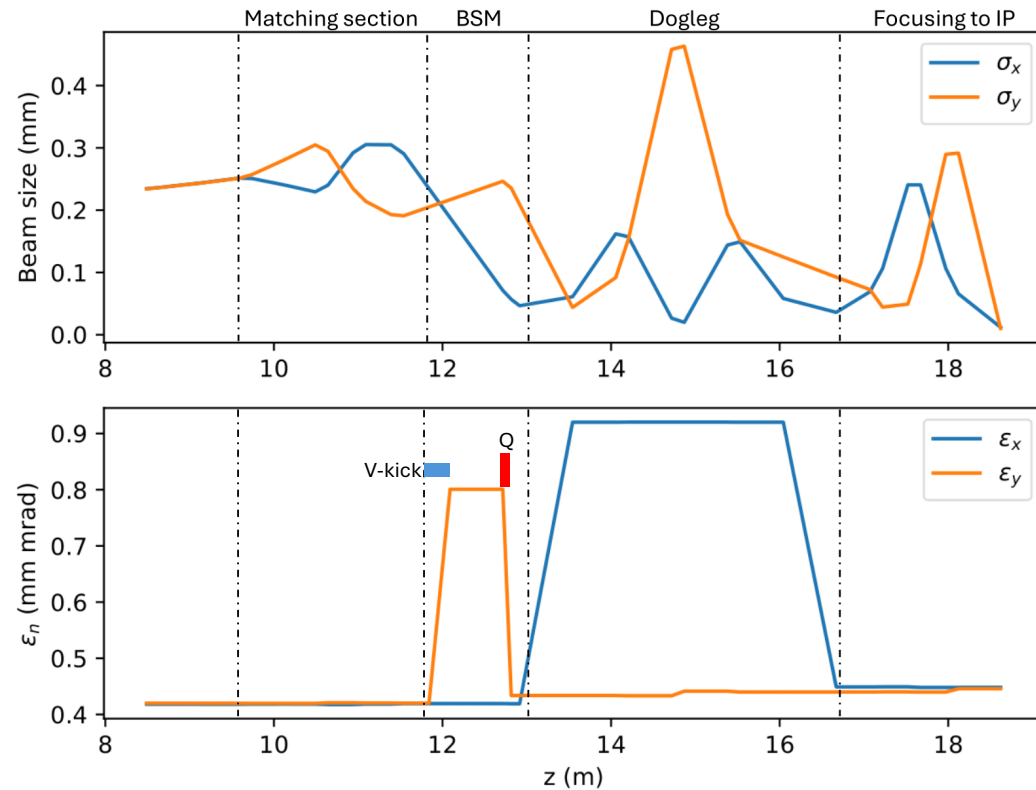
The doglegs are now **parallel**, but they lay on two different horizontal planes, **5.3 cm apart**, as their respective IPs.

Laminarity parameter along the beamline, measuring the relative importance of space charge effects vs. emittance pressure.

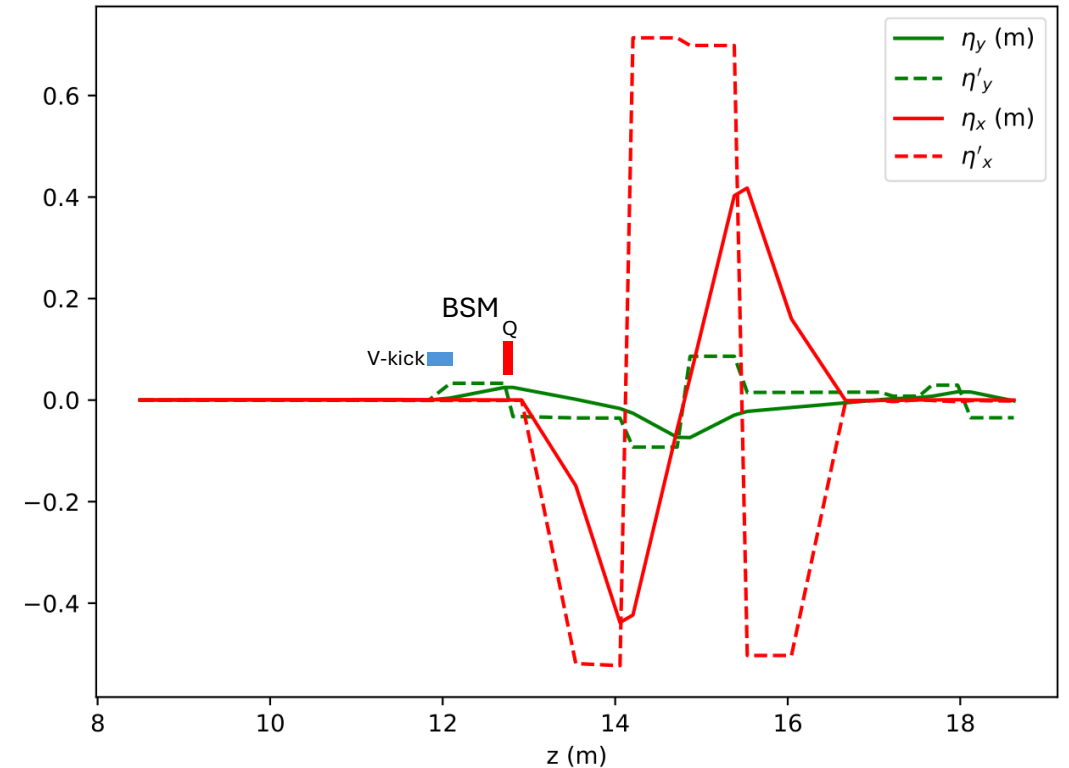


Beam transport and focusing to the IP

Beam dynamics simulation along the the beamline.



Dispersion functions along the beamline.



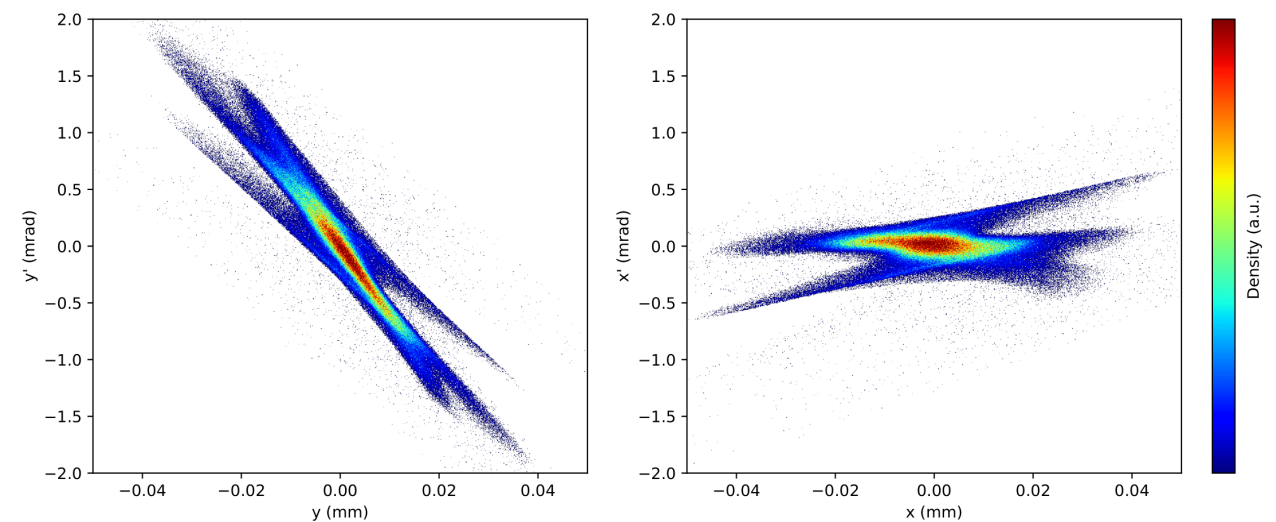
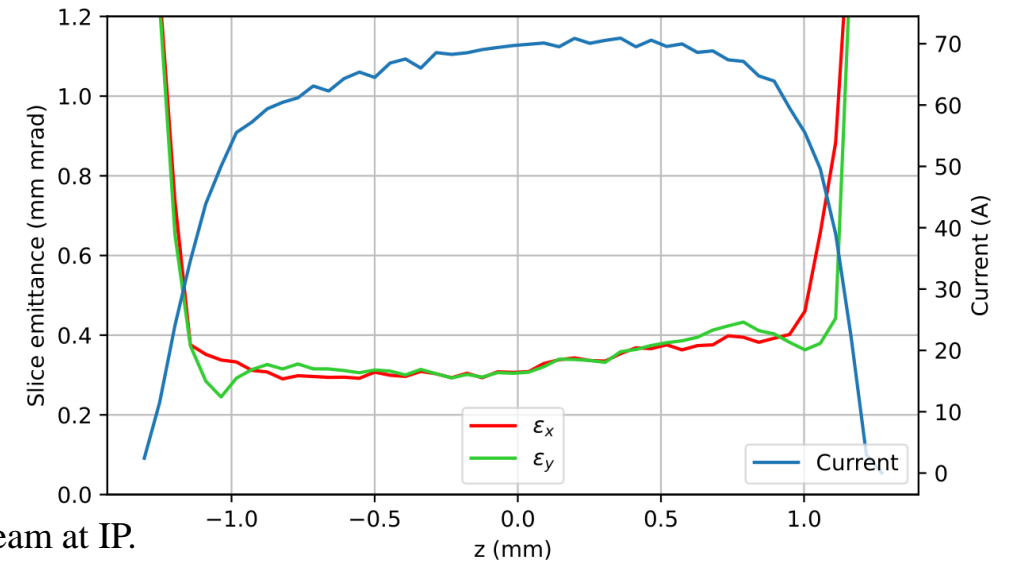
The BSM deflects the beam, acting as a vertical mini-dogleg and introducing a small **vertical dispersion** that cannot be corrected.

We studied a specific **matching** of the beam optics to the BSM that **minimise the dispersion contribution** to the vertical projected emittance.

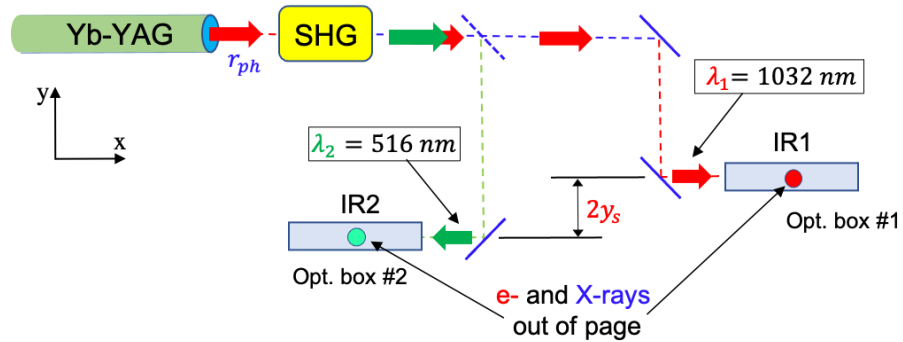
Beam parameters at the IP

Electron beam parameters at IP

Parameter	Value
Bunch charge [nC]	0.5
Beam energy [MeV]	145
Norm. proj. emittance [mm mrad]	0.45
Bunch length, rms [ps]	2.2
Horizontal beam size, rms [μm]	12.0
Vertical beam size, rms [μm]	10.0
Relative energy spread, rms [%]	0.03
Peak current [A]	71



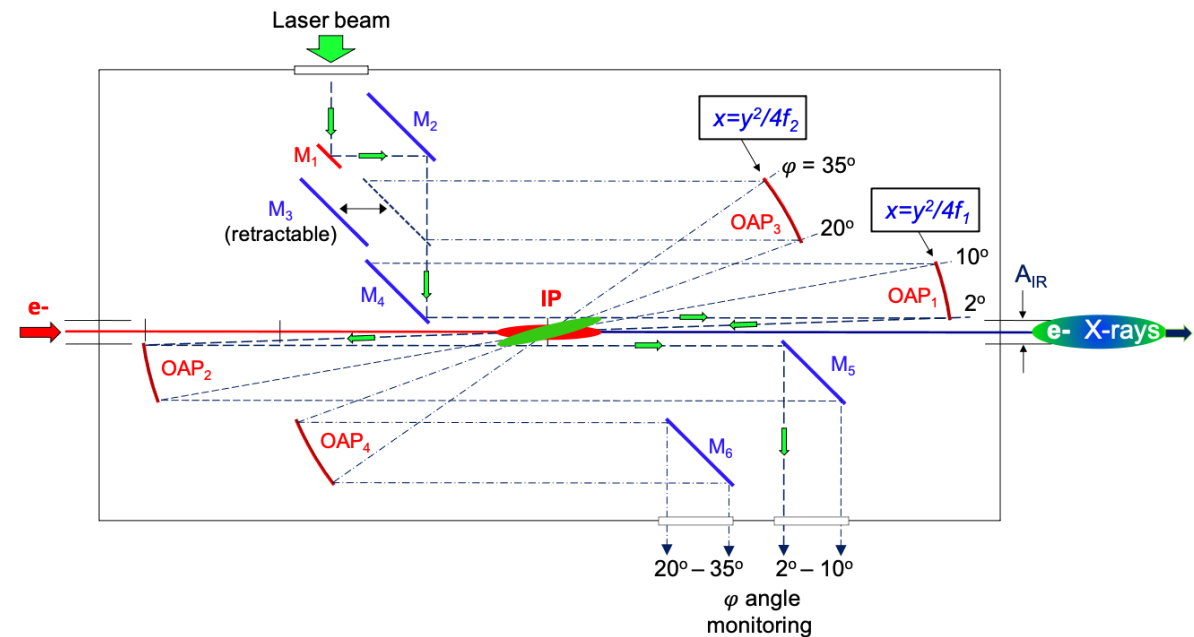
Laser and Optical box



Dual-frequency operation in the Multimode BoCXS scheme adopting Second Harmonic Generation (SHG). The optical boxes are vertically separated by the $2y_s=5.3$ cm offset.

Laser parameters at IP

Parameter	Value
Rep. rate [kHz]	0.1
Central wavelength [nm]	1032-516
Bandwidth, FWHM [%]	1
Beam quality factor	<1.5
Pulse energy [J]	1.0
Intensity pulse size, rms [μm]	10.0
Pulse duration, rms [ps]	3.0



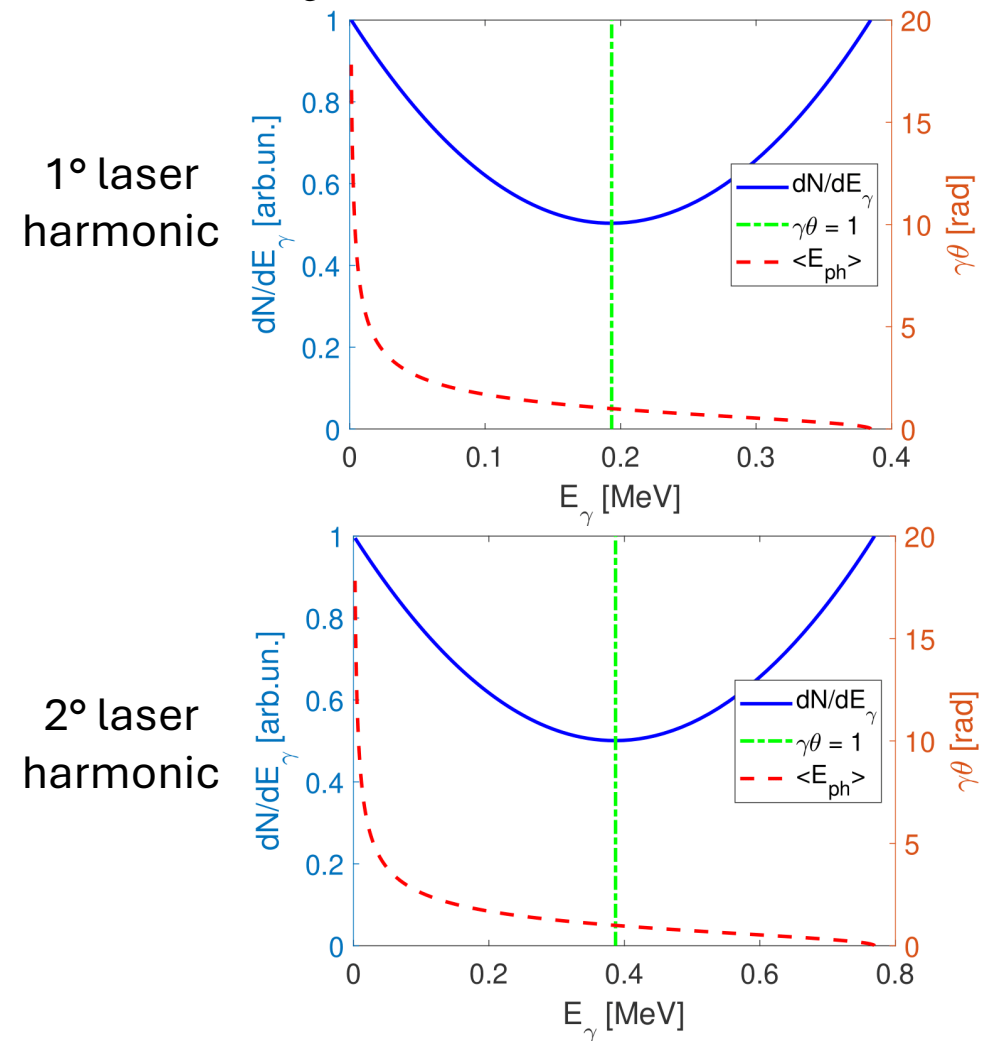
Layout of the optical box at one of the BoCXS laser-electron interaction regions. Two sets of OAP mirrors select the interaction angle φ within an operational range $\Delta\varphi_1 = 2^\circ - 10^\circ$ ($M_4 - OAP_1$) and a larger set $\Delta\varphi_2 = 20^\circ - 35^\circ$ ($M_3 - OAP_3$) to produce X-ray energy shifts of the order of 2–3 keV for KES dual-energy imaging. The angle φ is defined by the position of the scanning mirror M_1 and monitored through the $M_{5,6}$ extracting mirrors.

X-rays expected parameters

Compton X-ray expected parameters for an interaction angle of 2 deg (multimode operation)

Parameter	1° laser harmonic	2° laser harmonic
Rep. rate [kHz]	0.1	
Pulse duration, rms [ps]	1.85	
Source size, rms [μm]	5.9	
Source divergence, rms [mrad]	2.7	
Max. photon energy [keV]	383.7	768.6
Total peak intensity [ph/pulse]	$4.9 \cdot 10^8$	$1.9 \cdot 10^8$
Total peak power [W]	$5.4 \cdot 10^6$	$4.3 \cdot 10^6$
Total average intensity [ph/s]	$4.9 \cdot 10^{10}$	$1.9 \cdot 10^{10}$
Total average power [W]	$9.9 \cdot 10^{-4}$	$7.9 \cdot 10^{-4}$
Peak brilliance [ph/s/mm ² /mrad ² /0.1%BW]	$1.5 \cdot 10^{19}$	$5.9 \cdot 10^{18}$
Average brilliance [ph/s/mm ² /mrad ² /0.1%BW]	$6.8 \cdot 10^9$	$2.7 \cdot 10^9$
Average spectral density [ph/s/0.1%BW]	$7.3 \cdot 10^7$	$2.9 \cdot 10^7$

ICS intensity vs. photon energy (blue) and average photon energy vs. observation angle (red).



Ongoing activity



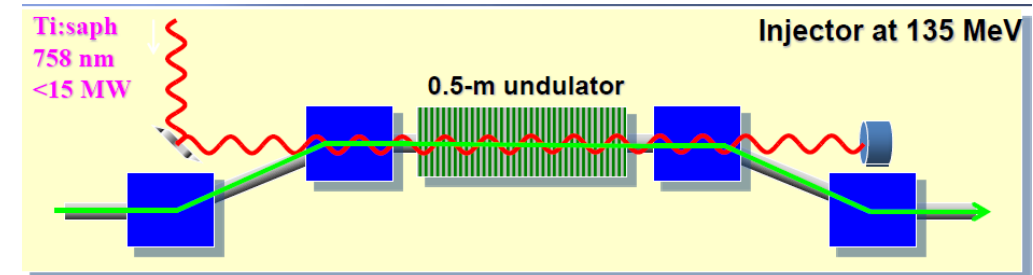
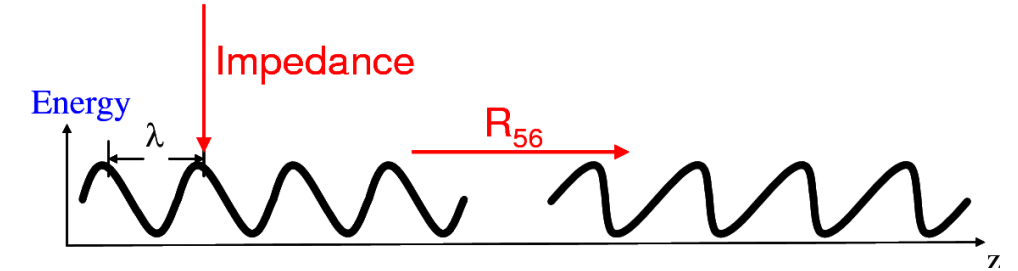
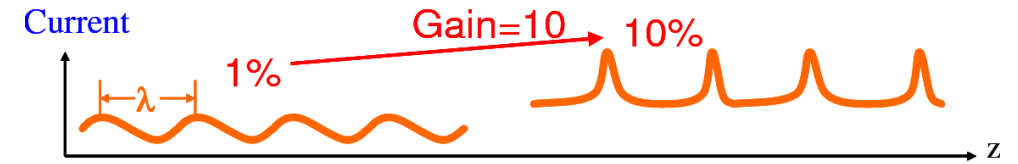
With the BoCXS project now on hold, we decided to apply the experience collected during these studies on a different topic.

Study the effects of **microbunching instabilities** (MBI) on X-ray Free-Electron Laser performance in the framework of EuPRAXIA@SPARC_LAB.

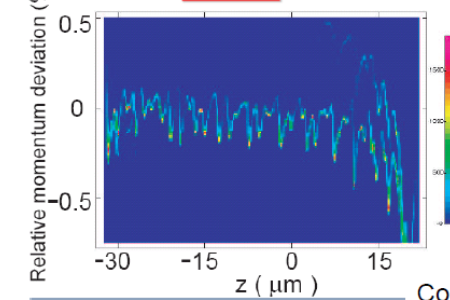
Possibility to use a **laser heater**, to provide a proper MBI mitigation through longitudinal Landau damping



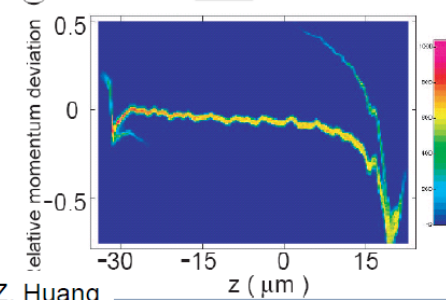
Elettra Sincrotrone Trieste



14 GeV Without Laser Heater



14 GeV With Laser Heater

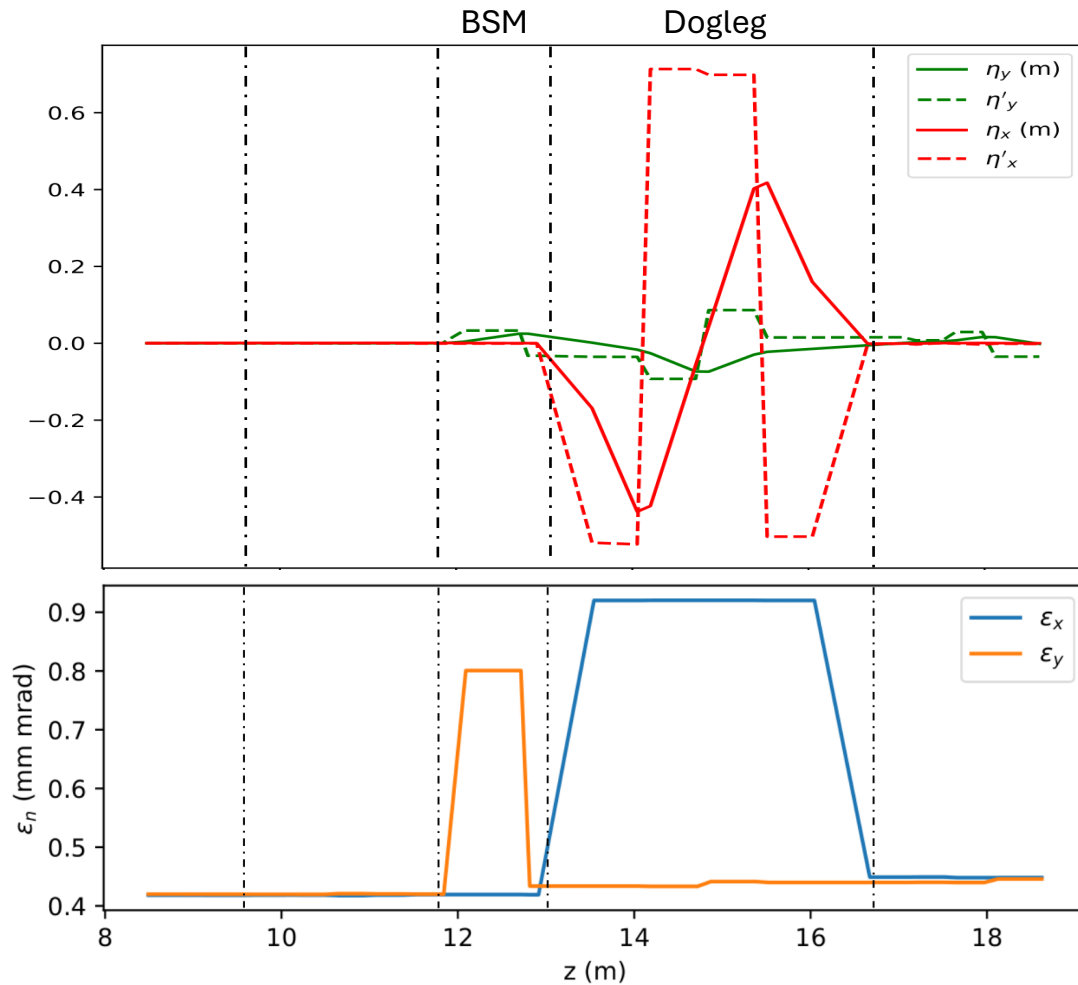


Courtesy of Z. Huang



Thank you for your attention

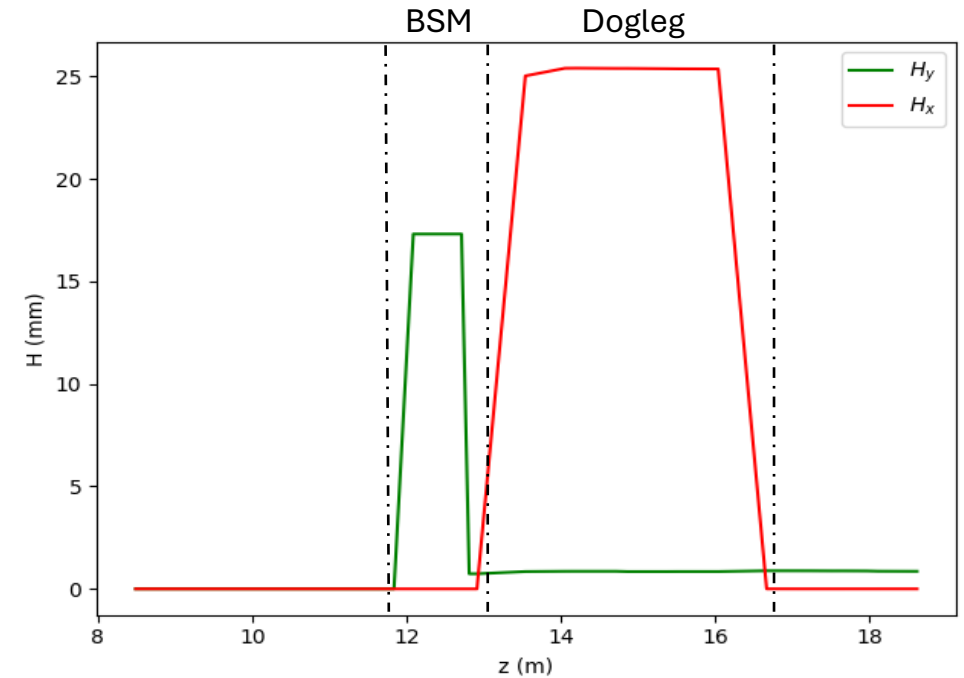
Dispersion contribution to the projected emittance



Dispersion functions (top) and beam projected emittance (bottom) along the beamline.

Chromatic \mathcal{H} -function

$$\gamma\eta^2 + 2\alpha\eta\eta' + \beta\eta'^2 = \mathcal{H}$$



\mathcal{H} -functions along the beamline.

SIMULATIONS

Simulation with space charge effects (start to end).

Stability studies (errors, jitters...).

Simulation of inverse Compton scattering.

Characterisation of the X-ray beam for specific applications.

